JOURNAL OF GUIDANCE, CONTROL, AND DYNAMICS
Vol. 30, No. 6, November–December 2007

Effect of Wind Correlation on Aircraft Conflict Probability

Georgios Chaloulos* and John Lygeros†
Swiss Federal Institute of Technology (ETH), 8092 Zurich, Switzerland

DOI: 10.2514/1.28858

A study which examines the effect of wind correlation on aircraft conflict probability estimation is presented. We describe the correlation structure of the difference between the actual wind and the meteorological wind forecasts and discuss how it can be implemented in simulation. For several encounters we then examine the aircraft conflict probability estimation errors if the correlation structure is ignored and the wind is instead assumed to be modeled as white noise. The conclusion of the study is that wind correlation may have a significant effect under particular encounter geometries.

Nomenclature

f_i	=	individual correlation functions
h	=	flight altitude
k_1, k_2	=	gains of the bank angle controller
$O(i)$	=	way point i
$P(t)$	=	three-dimensional position of the aircraft at time t
R	=	correlation matrix
r_{xy}	=	covariance function
t_{conflict}	=	time to minimum separation
V	=	true airspeed
w	=	wind speed vector
X	=	x coordinate of the aircraft
Y	=	y coordinate of the aircraft
$\delta(t)$	=	cross track deviation at time t
$\delta_{\min}$	=	minimum separation
ϵ	=	estimation error
$\Theta(t)$	=	heading error at time t
θ	=	crossing angle
σ	=	wind standard deviation
ϕ	=	bank angle
$\Psi(i)$	=	reference heading at way point i
ψ	=	heading angle

I. Introduction

THE increasing demand for air travel is beginning to stress the air traffic management (ATM) system to its limits. A potential solution to this problem can be the use of computational tools to simplify the tasks of human operators [1]. Examples of such computational tools are conflict probes, which predict proximity conflicts and inform the air traffic controller (ATC). These tools can help the operators handle the increased demand more reliably, increasing safety and efficiency levels. The algorithms might even evolve into completely automated tools, taking over decisions for simple ATC tasks, allowing controllers to concentrate on strategic decisions that improve the efficiency of the system. Numerous tools have been proposed in this direction [2], predicting conflict situations and/or proposing resolution maneuvers either to the ATC or to the pilots.

Received 14 November 2006; revision received 27 February 2007; accepted for publication 8 March 2007.

*Doctorate Student, Department of Information Technology and Electrical Engineering, Automatic Control Laboratory, Physikstrasse 3; chaloulos@control.ee.ethz.ch.

†Professor, Department of Information Technology and Electrical Engineering, Automatic Control Laboratory, Physikstrasse 3; lygeros@control.ee.ethz.ch.

A key difficulty in the design of conflict probes is the uncertainty that enters the prediction of the future positions of aircraft. Much of this uncertainty is due to weather conditions, which pose two problems. First, hazardous weather causes aircraft to maneuver around hazardous convective weather cells and thus makes it uncertain when an aircraft will be in conflict with other aircraft. Second, weather forecast uncertainties cause errors in conflict prediction. The exact impact of the weather conditions that aircraft experience on the predictions of conflict probes and on aircraft trajectories is not well understood. One component of the weather that greatly affects an aircraft trajectory is the wind. The wind mostly affects a trajectory through its speed. In general, the wind speed can be modeled as a sum of two components: a nominal, deterministic component (available through meteorological forecasts) and a stochastic component, representing deviations from the nominal. Conflict probes differ in the way they take the wind into account. Some treat the wind as completely deterministic. Here the wind experienced by the aircraft is assumed to be known before the flight (exactly following the forecasts). Other probes treat the wind as completely stochastic, where the wind is modeled as a random variable [3,4]. Finally, some probes do both [5,6].

Probes that involve a stochastic wind component again differ in the way they take into account the spatiotemporal correlation of the wind such as follows:

1) Uncorrelated, where the wind samples extracted for each aircraft are not correlated with previous wind samples or near wind conditions [7,8].

2) Correlated in space but not time [9].

3) Correlated in both time and space, which is the most general case [3,4,10].

4) Uncorrelated between different aircraft, where each aircraft flies in a separate wind field, each one correlated in time and/or space [5,6,11–13].

There is no consensus as to the impact of wind correlation on the reliability of conflict probes. Some authors claim it is important [13], others that it is not [9,11]. We will attempt to quantify the effect of wind correlation using Monte Carlo simulation of a model that includes a full spatiotemporal correlation structure of the wind [14] in many different scenarios, using wind speed uncertainty of the rapid update cycle 40 km (RUC-2) forecast model. A related study based on less accurate RUC-1 [15] suggests that wind correlation has a significant effect under particular encounter geometries.

In this paper, Sec. II presents an overview of the model used in our simulations and a closer examination of the properties of the wind correlation structure. Section III discusses the tuning of the simulator parameters to match experimental data. Section IV demonstrates the results of the simulations conducted in different conflict scenarios and, finally, Sec. V states the conclusions of this research.

II. Model Overview

To perform the simulations, we have appropriately modified the model developed in [14]. In this section we describe these modifications.

The model allows one to capture multiple flights taking place at the same time. Each flight has a flight plan, aircraft dynamics, and a flight management system (FMS). The evolution of flights is affected by the weather; currently the only aspect of weather modeled is the wind speed. The effect of the measurement errors, arising because of the sensor noise, is also taken into consideration. We model the wind speed as a sum of two components: nominal and stochastic. The stochastic component is assumed to be zero mean and correlated in space and time. Therefore, the evolutions of different flights are coupled to one another through the wind model; recall that the wind components are correlated between all simultaneous flights.

The work is framed in the context of stochastic hybrid processes. In particular, the model comprises the following:

1) Deterministic dynamics, which can be divided in continuous dynamics, arising from the physical motion of the aircraft and discrete dynamics, arising from the flight plan and the logic variables embedded in the FMS.

2) Stochastic dynamics, arising from the wind and the sensor noises.

A. Aircraft Dynamics

The aircraft is modeled using a point mass model (PMM), based on the base of aircraft data (BADA) database [16]. Apart from the continuous dynamics, discrete dynamics also arise in our model, mainly because of the FMS and the flight plan.

The flight plan consists of a sequence of way points $\{O(i)\}_{i=0}^{M}$, in three dimensions, $O(i) \in \mathbb{R}^3$. The sequence of the way points defines a sequence of straight lines joining each way point to the next; we call this the reference path. In our experiments, the requested time of arrival (RTA) for each way point is not included. As a result, the aircraft can only correct cross track deviations from the reference path and along-track errors are ignored. This assumption reflects what is known as a 3-D FMS; this is currently the standard for commercial aircraft, because not all aircraft are yet equipped with an FMS better than 3-D.

The FMS can be thought of as a controller, which, by measuring the state and using it together with the flight plan, determines the values for the inputs. The control is to some extent continuous, but some parameters and set points of the controllers depend on the discrete dynamics of the FMS [14].

B. FMS Controller

The FMS controller [14] is divided in two components: one that determines the along-track and vertical motions through the thrust and the flight path angle, and the other controlling cross track motion through the bank angle. Here we provide details only on the cross track crontroller, because its parameters will be used later.

The model we use assumes that the FMS sets the bank angle based on the heading error and the cross track deviation from the reference path. The controller operates in continuous time and consists of a linear feedback part, followed by nonlinearities to ensure that the behavior is reasonable even with extreme inputs. The geometry of the situation is summarized in Fig. 1. For each way point $O(i)$, we define the reference heading $\Psi(i)$ as the angle that the line segment joining $O(i)$ to $O(i+1)$ makes with the X axis of the frame in which the way-point coordinates are given. At time t, we denote by $P(t) = (X(t), Y(t), h(t))$ the 3-D position of the aircraft and assume that it is moving between way points i and $i+1$. The heading error is then

$$\Theta(t) = \Psi(i) - \psi(t) \tag{1}$$

and the cross track deviation is

$$\delta(t) = [-\sin\Psi(i) \quad \cos\Psi(i) \quad 0](P(t) - O(i)) \tag{2}$$

The linear part of the controller is given by

$$\phi_1(t) = k_1\delta(t) + k_2\Theta(t) \tag{3}$$

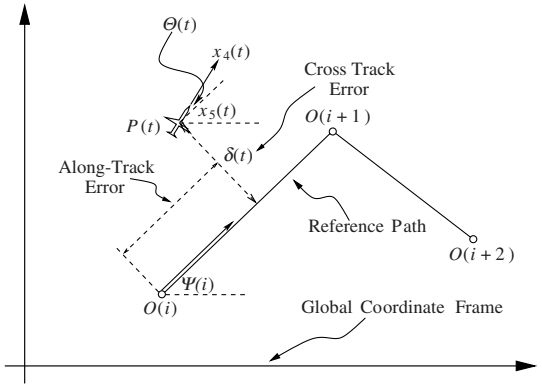

Fig. 1 Geometry for calculating cross track and heading errors.

Stability reasons demand that both k_1 and k_2 are negative [14]. The values of the gains k_1 and k_2 are set to generate realistic cross track deviation statistics; see Sec. III.B.

The linear controller may command unrealistically large bank angles in cases where large deviations from the reference path are observed. To prevent this, a saturation value at the angle $\bar{\phi} = 35$ deg is introduced.

$$\phi_2(t) = \begin{cases} -\bar{\phi} & \text{if } \phi_1(t) \le -\bar{\phi} \\ \phi_1(t) & \text{if } -\bar{\phi} \le \phi_1(t) \le \bar{\phi} \\ \bar{\phi} & \text{if } \phi_1(t) \ge \bar{\phi} \end{cases} \tag{4}$$

Even with the saturation, the aircraft may fail to converge to the reference path if it deviates too far from it and may instead travel in circles. For this reason we introduce a further limit on the bank angle as a function of the heading error. Thus, the final setting for the bank angle is

$$\phi(t) = \begin{cases} \min\{\phi_2(t), 0\} & \Theta(t) \ge \bar{\psi} \\ \phi_2(t) & -\bar{\psi} < \Theta(t) < \bar{\psi} \\ \max\{\phi_2(t), 0\} & \Theta(t) \le -\bar{\psi} \end{cases} \tag{5}$$

In the simulations $\bar{\psi} = 60$ deg is used.

This controller is used both for tracking straight lines and for turning from one leg of the reference path to the next [14].

C. Stochastic Dynamics

The stochastic terms of our model arise mainly because of 1) the wind velocity, 2) the airspeed measurement errors of the aircraft, and 3) the air temperature uncertainty.

1. *Stochastic Wind Model*

The wind velocity is modeled as a sum of two terms: a deterministic (nominal) component, representing the meteorological predictions available to ATC and a stochastic component, representing inaccuracy and uncertainty in these predictions. Because the meteorological predictions are known and available to the ATC before a flight takes place, the flight plans, the way points, and the requested time of arrival for each way point are adjusted taking into consideration the predictions. Thus, the way the nominal wind affects aircraft trajectories is deterministic and known a priori. Because we are interested in the effect of stochastic deviations from nominal wind (in particular, their correlation structure), we set the deterministic part of the wind to zero for simplicity.

The stochastic wind component is modeled as a random field w: $\mathbb{R} \times \mathbb{R}^3 \to \mathbb{R}^3$, where $w(t, P)$ represents the wind at point $P \in \mathbb{R}^3$ and at time $t \in \mathbb{R}$. We assume that $w(t, P)$ is a Gaussian random variable with zero mean. Recall that the wind experienced by each aircraft at a given time is correlated to the wind experienced by all other aircraft at the same time and the wind experienced by all aircraft at earlier times. A detailed procedure for extracting wind samples with given spatiotemporal correlation can be found in [14]. Here we

just give the formulas for the correlation structure of the stochastic part of the wind.

Under the assumption that for all t, P, $w(t,P)$ is zero mean, let $R(t,P,T',P') = E[w(t,P)w(t',P')^T]$ for t, $t' \in \mathbb{R}$ and P, $P' \in \mathbb{R}^3$. Then under mild assumptions [14]

$$R(t,P,T',P') = \begin{pmatrix} r_{xy}(t,P,T',P') & 0 & 0 \\ 0 & r_{xy}(t,P,T',P') & 0 \\ 0 & 0 & r_z(t,P,T',P') \end{pmatrix} \quad (6)$$

The most relevant source of information about the properties of function R is [17]. Excluding situations such as wind shear, the vertical component of the wind $w_3(t,P)$ will be small compared to the horizontal component $\sqrt{w_1^2 + w_2^2}$. It is reasonable then to assume that $w_3(t,P) = 0$ to simplify computations. The covariance function for the horizontal wind terms implemented in the simulator has the following form:

$$r_{xy}\left(t, \begin{bmatrix} X \\ Y \\ h \end{bmatrix}, t', \begin{bmatrix} X' \\ Y' \\ h' \end{bmatrix}\right) = \sigma_{\text{model}}(h)\sigma_{\text{model}}(h') f_t(|t-t'|) f_{XY}\left(\begin{vmatrix} X-X' \\ Y-Y' \end{vmatrix}\right) f_h(|p(h)-p(h')|) \quad (7)$$

Here $p(\cdot)$ is the following function, giving the air pressure in millibars (mb) at a specific altitude in meters, assuming a standard atmosphere:

$$p(h) = 288.08\left(\frac{-0.00649h + 288.14}{288.08}\right)^{5.256} - 273.1 \quad (8)$$

Data [17] suggest the following individual correlation functions:

$$f_t(x) = 0.154 + 0.7755e^{-\frac{x}{11,850}} + 0.0705\cos\left(2\pi\frac{x - 32,640}{76,500}\right) \quad (9)$$

$$f_{XY}(x) = -0.006 + 1.006e^{-\frac{x}{337,000}} \quad (10)$$

$$f_h(x) = -0.1 + 1.1e^{-\frac{x}{213}} \quad (11)$$

The selection of the standard deviation value is discussed in Sec. III.A. Figures 2–4 show the variation of the individual correlation functions. Notice that $f_t(0) \neq 1$. This is because the stochastic part of the wind is not accurately known at this time; further discussion can be found in [17].

2. *Measurement Errors and Air Temperature Uncertainty*

Two other sources of uncertainty for an aircraft trajectory are the airspeed measurement errors and the uncertainty about air temperature [11]. Both result in deviations from the flight plan in the along-track directions.

For airspeed measurement errors, the airspeed indicators typically have errors which result in a standard deviation of 5 kt to the airspeed. Because the error is mostly depending on the indicator, for each aircraft we assume this error is random, constant in time, and uncorrelated to the errors of other aircraft. We assume that this airspeed error is fully correlated in time for a given aircraft (i.e., the airspeed error is considered constant for a single flight, but independent for different aircraft).

For the temperature uncertainty, even the best available temperature forecasts have a standard deviation of about 2 K, which gives rise to speed errors of about 2 kt. We again assume for simplicity that this error is for each aircraft random, constant in time,

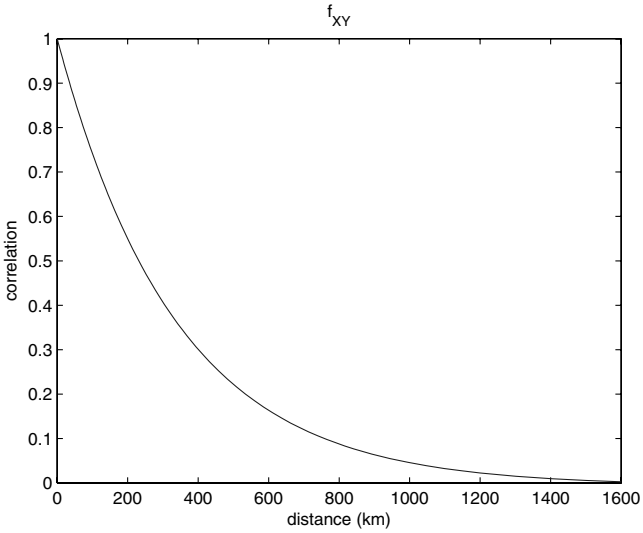

Fig. 2 Horizontal correlation as a function of distance.

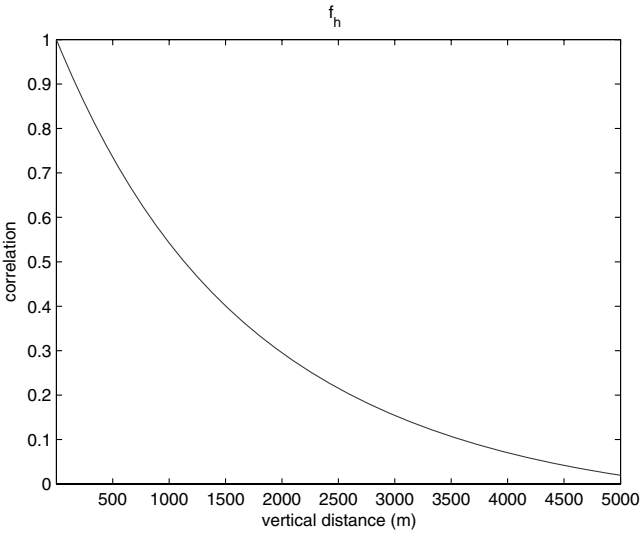

Fig. 3 Vertical correlation as a function of distance.

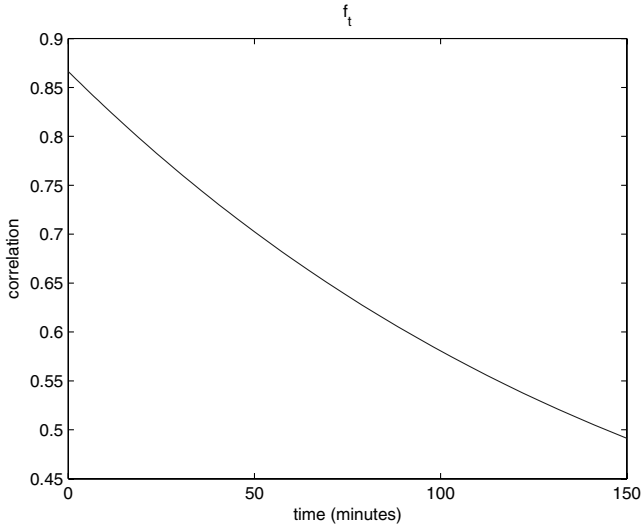

Fig. 4 Time correlation as a function of time.

Table 1 Estimate of the standard deviation of the error in RUC-2 forecasts (in ms^{-1})

Pressure, mb	$\sigma_{\text{fcst-ACARS}}$	σ_{ACARS}	σ_{model}
900–800	5.58	2.45	5.01
800–700	5.39	2.12	4.96
700–600	5.15	2.12	4.75
600–500	4.85	1.87	4.48
500–400	4.86	1.73	4.54
400–300	4.84	1.58	4.57
300-200	5.45	1.73	5.17
200–100	5.67	1.87	5.35

and uncorrelated to the errors of other aircraft. It seems rational to assume that it is highly correlated (constant) in time, because if an aircraft encounters a temperature deviation from the predictions, it will probably continue encountering it for a time period. Omitting the correlation of temperature errors between aircraft, though, underestimates the total effect of the correlation of all weather aspects.

It is assumed that both speed measurement errors and temperature errors are zero mean and Gaussian $N(0, \sigma_{\text{speed}})$ and $N(0, \sigma_{\text{temperature}})$ and assuming that the two errors are independent, we get a resulting standard deviation for the airspeed error

$$\sigma^2_{\text{total}} = \sigma^2_{\text{speed}} + \sigma^2_{\text{temperature}} \tag{12}$$

We can now model the error as a bias added to the airspeed of each aircraft $\Delta\upsilon \sim N(0, \sigma_{\text{total}})$. From Eq. (12) we get a resulting standard deviation of 5.38 kt.

III. Tuning of the Model

We tune the model to simulate enroute encounters. Thus, we use data found in the literature concerning the wind standard deviation and the along-track and cross track errors for a typical cruising altitude.

A. Selecting Wind Standard Deviation

The data collected by aircraft communications, addressing, and reporting system (ACARS) observations suggest that the wind speed deviations from the forecasts of RUC-2 have a standard deviation of $\sigma_{\text{fcst-ACARS}}$ given in Table 1 [18]. Although this might seem accurate, we cannot ignore errors in the ACARS observations [19], which become enmeshed with wind field errors:

$$\sigma^2_{\text{fcst-ACARS}} = \sigma^2_{\text{ACARS}} + \sigma^2_{\text{model}} \tag{13}$$

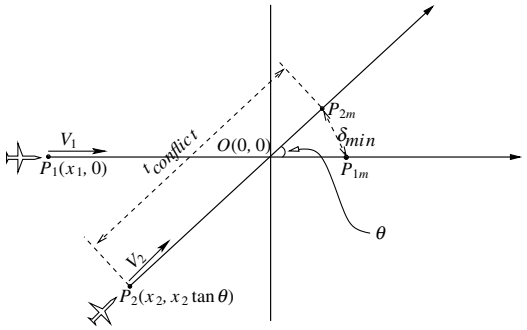

Fig. 6 Level flight conflict scenario.

where σ_{ACARS}, σ_{model} represent the standard deviations of the ACARS observation errors and the RUC-2 model forecasts errors, respectively. Equation (13) holds, because observation errors and forecast errors at the time of those observations are independent and, thus, the covariance between them is zero [17,18].

Using Eq. (13) and σ_{ACARS} estimates [19], we get σ_{model} (Table 1), which we use in our model.

B. Tuning of the FMS Parameters

After selecting the wind standard deviation, we have to tune the control parameters k_1 and k_2 to reproduce results suitable for real flights. Studies have shown that in enroute airspace the variance of the along-track position error grows quadratically in time and the variance of the cross track position error grows quadratically up to a maximum value and then saturates [20]. By contrast, [5] suggests that along-track variance grows in a linear way, rather than quadratically.

Because we assume a 3-D FMS, we expect the along-track errors to be completely determined by the wind statistics and the speed measurement errors. Cross track position errors on the contrary are controlled by the FMS gains k_1 and k_2.

In the case of the full correlated wind model, as shown in [14], if the wind is stochastic, but changes slowly, we expect the standard deviation of the cross track position error to be approximately

$$\frac{k_2\sigma}{k_1 V} \tag{14}$$

where σ denotes the wind standard deviation and V the airspeed. Equation (14) suggests that the steady-state cross track error could be set by selecting the ratio of k_1 and k_2. Monte Carlo simulation shows that the growth rate does not vary much with k_1 and k_2, so we are left

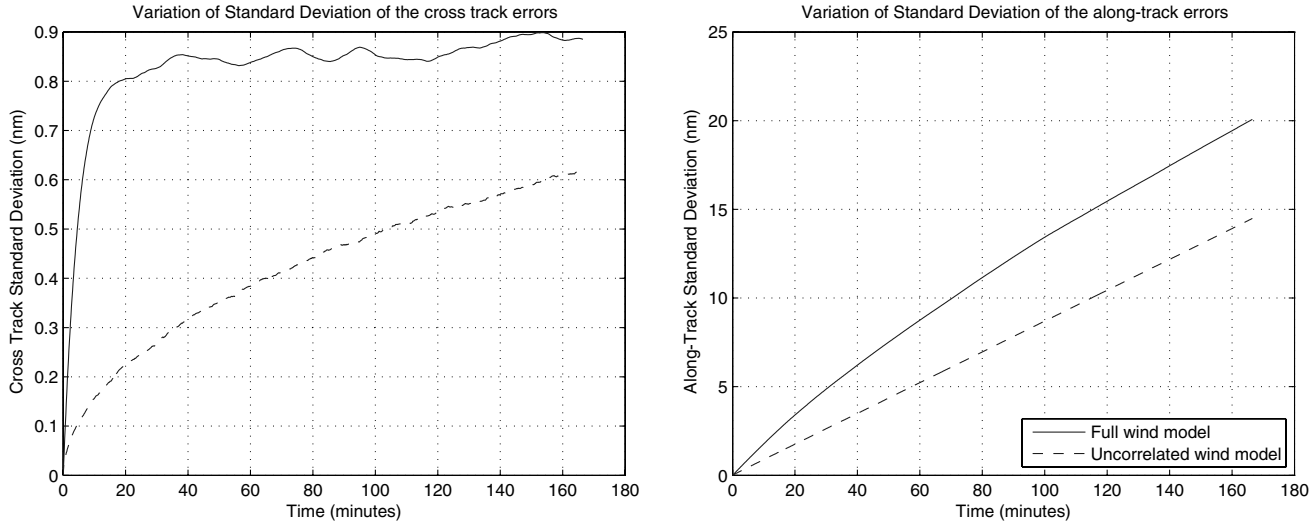

a) Cross Track Errors **b) Along-Track Errors**

Fig. 5 Variation of the standard deviation of the cross track and along-track errors.

with some degree of freedom when choosing the gains. Thus, a large value for k_2 is selected, as it tends to give better performance when the aircraft is turning from one leg of the reference path to the next. The saturation value of the cross track deviation varies, depending on whether the aircraft is equipped with an FMS or not. Several figures can be found in different references: 0.5 nm [13] and 0.39 nm [21] for aircraft equipped with FMS, "more than 1 nm" for non-FMS equipped aircraft [13], 1 nm [22] or 2 nm [23] for a mix of aircraft, while other studies suggest that empirically the cross track error keeps growing to beyond 4 nm [5]. As aircraft technology advances, these values are likely to become smaller. We choose 1 nm as the saturation value to use in Eq. (14). For a typical cruising speed, the

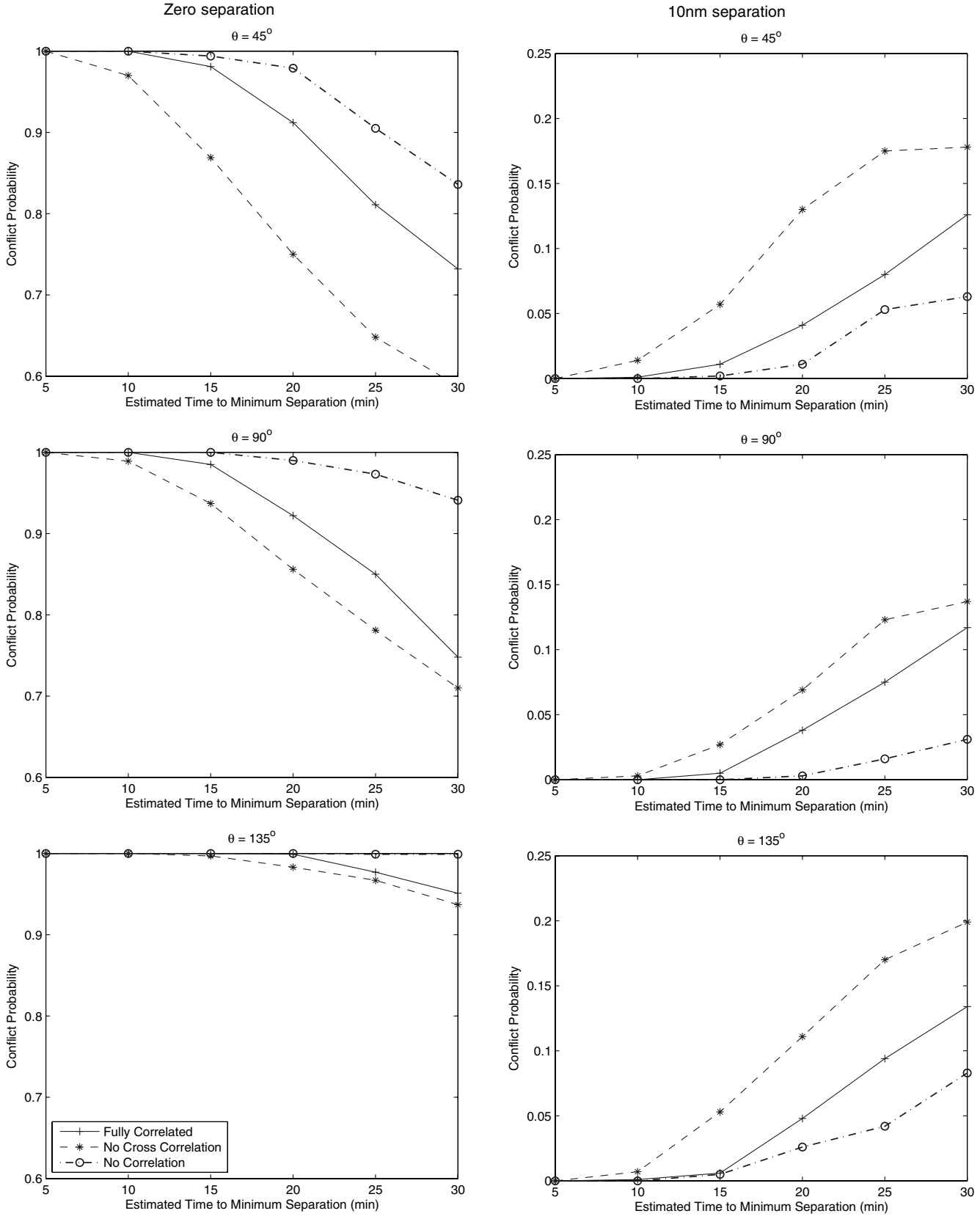

Fig. 7 Effect of wind correlation on conflict probability for level flight scenarios.

values of k_1 and k_2 then become

$$k_1 = -1 \times 10^{-5} \text{ rad} \cdot \text{m}^{-1} \tag{15}$$

$$k_2 = -\frac{1 \text{ nm} \cdot k_1 \cdot 240 \text{ ms}^{-1}}{5 \text{ ms}^{-1}} = -0.89 \tag{16}$$

Figure 5 shows the variation of the standard deviations of the cross track and along-track position errors with respect to time for an aircraft flying in a straight line at cruising altitude with the k_1 and k_2 calculated above, obtained by 10,000 Monte Carlo simulations. We can see that the cross track error levels out at a saturation value of roughly 0.85 nm within the first 15 min. Regarding the along-track error, we can see that the growth rate is roughly linear and, in the first 15–20 min the growth rate matches the one described in [5] (about 0.25 nm/ min). Over a longer time horizon the along-track growth rate decreases to about 0.135 nm/ min, matching the growth rate suggested in [11]. The higher deviations reported in [5] are justified due to the fact that we completely ignore the deterministic part of the wind and that the results of [5] are based on measurements of aircraft flying at different cruising altitudes, leading to a variety of airspeeds and, consequently, higher growth rates of the standard deviation.

The previous discussion does not apply in the case of wind not correlated in time and space. We tried to use the same bank angle control for this case. To match the statistical data of [5], we tried to properly tune the control parameters k_1 and k_2. This was not possible, because the uncorrelated wind leads to much smaller deviations. This is why in this case we set both control parameters equal to zero. Figure 5 also shows the standard deviations of the cross track and along-track errors as before, with the use of random, uncorrelated wind instead of the correlated model. We observe that even with no bank angle control the deviations are still lower than the growth rates suggested in the literature. The linear growth of the standard deviation in the along-track error is explained by the fact that in this case the error is dominated by the airspeed measurement errors and the temperature uncertainty, which are kept constant during each simulation.

IV. Simulation Results

To produce a quantitative estimate of the effect of the correlation of the wind fields on the trajectory prediction, experiments with various conflict scenarios between two aircraft were simulated as follows:

1) Level–level is the most usual case found in the literature, where both aircraft cruise at the same altitude, and a fairly common encounter in practice [11] (Sec. IV.A).

2) Level–climb and level–descent, where one aircraft is cruising and the other one climbing or descending. This is the most usual three-dimensional conflict scenario [11] (Sec. IV.B).

3) Climb–descent, where one aircraft is climbing and the other is descending (Sec. IV.C).

4) Takeoff, where one aircraft is taking off. This is the case where the effect of the correlation in the wind field should be minimal, since the initial altitude difference takes a larger value (Sec. IV.D).

Another conflict scenario is the case where both aircraft are in the same phase of flight, climbing or descending. These are the most rare scenarios [11], with only 5% of the total conflicts occurring with both aircraft climbing and 4% with both aircraft descending. These cases are not included in this study.

We consider three different cases, concerning the correlation in the wind fields, as follows:

1) Full correlation model: In this case simulations are run with the full correlation model described in Sec. II.C.

2) No cross-correlation model: In this case, the wind experienced by each aircraft is considered to be correlated in time and space, but there is no correlation between the wind fields that different aircraft experience.

3) No correlation model: This is the case where the correlation function is completely ignored and the wind speed is assumed to be given at each moment by a zero-mean Gaussian random number, with the standard deviation calculated in Sec. III.A.

In the first two cases the gains k_1 and k_2 are set equal to the values determined in Sec. III.B. In the last case we set $k_1 = k_2 = 0$.

To estimate the effect of wind correlation, we perform Monte Carlo simulations and estimate the conflict probability of the aircraft by performing 1000 simulations and computing the fraction of them that enters conflict. By the term conflict we define a situation where two aircraft violate required minimum separation standards, in our case 5 nm horizontally and 1000 ft vertically. We consider three different crossing angles $\theta = (45, 90, 135 \text{ deg})$, six different values for nominal time to minimum separation $t_{\text{conflict}} = (5, 10, 15, 20, 25, 30 \text{ min})$, and two different nominal minimum separations $\delta_{\text{min}} = (0, 10 \text{ nm})$ (see Fig. 6). To compare the results from each case, we define the absolute estimation error as the absolute value of the difference of the two conflict probabilities:

$$\epsilon(t_{\text{conflict}}, \theta, \delta_{\text{min}}) = |CP_{\text{cm}}(t_{\text{conflict}}, \theta, \delta_{\text{min}}) - CP_{\text{em}}(t_{\text{conflict}}, \theta, \delta_{\text{min}})| \tag{17}$$

where $CP(t_{\text{conflict}}, \theta, \delta_{\text{min}})$ stands for the conflict probability at time t_{conflict}, crossing angle θ and minimum separation δ_{min}, and the indexes "cm" and "em" stand for the correlated model and the estimated model used, respectively.

A. Level–Level Encounters

According to statistical data [11] only 17% of conflicts are likely to happen with both aircraft flying level. This fact is used in many studies to justify neglecting the correlation in the wind field. On the other hand, more than half of the studies use two-dimensional conflict probes [2], where the correlation should have a greater impact, because the correlation in the vertical direction decays rather rapidly.

We consider two aircraft flying level at the same altitude, in straight lines, at constant airspeeds (see Fig. 6). In the absence of a wind field, the two aircraft approach each other at a specific distance δ_{min} after a specific time t_{conflict} (time to minimum separation). This is the minimum distance that the aircraft would approach if no wind was present.

We construct flight plans to code this encounter geometry to intersect at $O(0, 0)$. $P_1(t) = (x_1(t), 0)$ and $P_2(t) = (x_2(t), x_2(t) \tan\theta)$ denote the positions of the aircraft at time t. We use two different values for the minimum separation δ_{min}: zero (zero minimum separation) and 10 nm (nonzero separation). Even though nominally the aircraft would follow exactly their flight plans, uncertainty in aircraft motion forces them to a different minimum

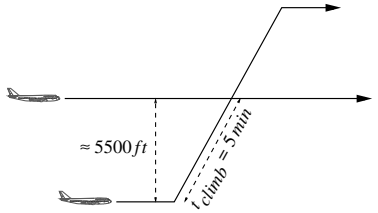

Fig. 8 Conflict scenario with one aircraft flying level and one climbing.

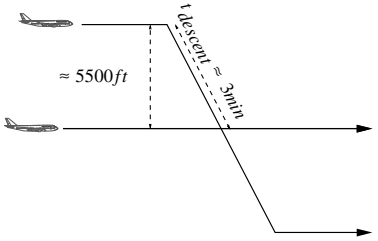

Fig. 9 Conflict scenario with one aircraft flying level and one descending.

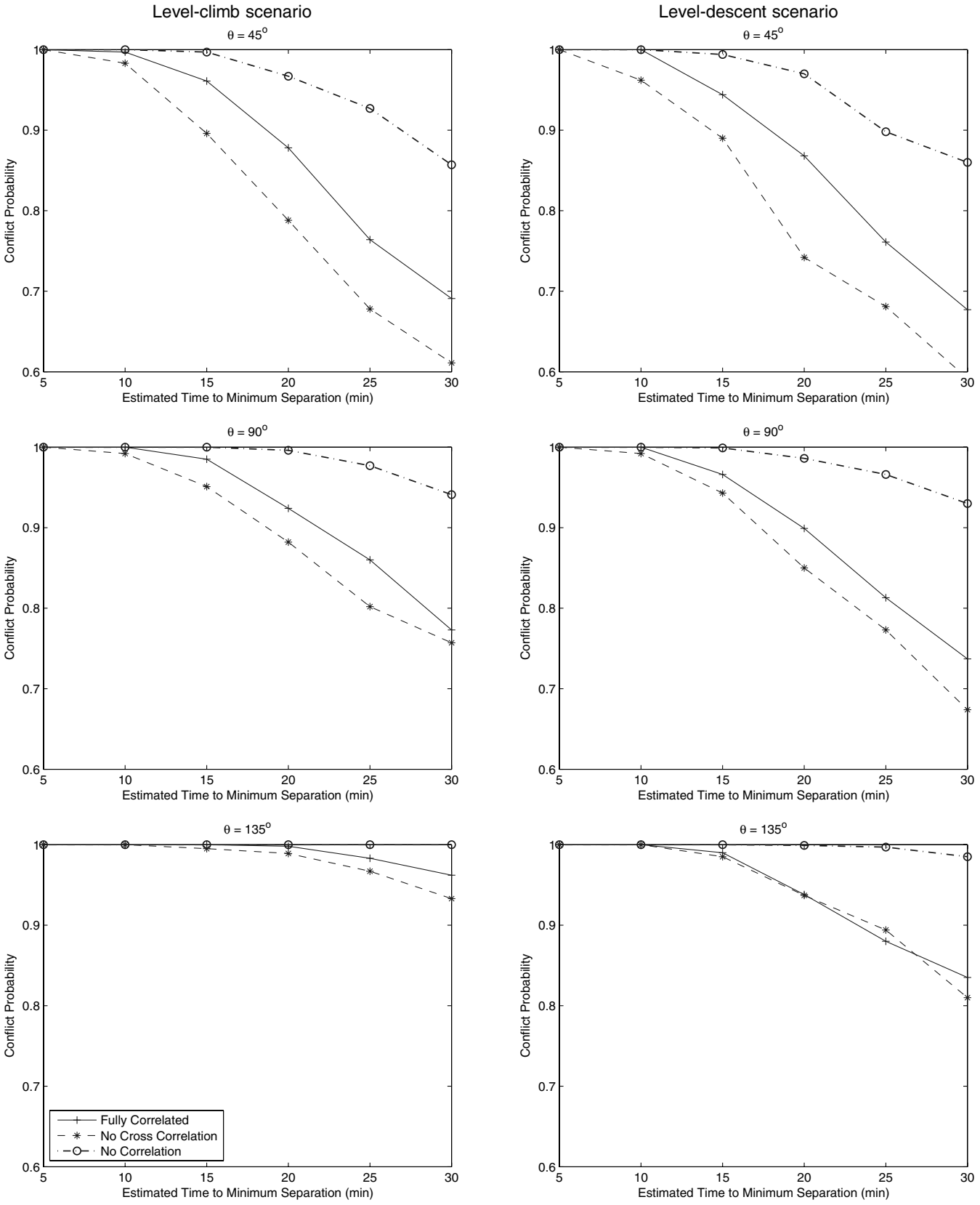

Fig. 10 Effect of wind correlation on conflict probability for level–climb and level–descent flight scenarios.

separation at a different time, and thus, t_{conflict} is the estimated time to minimum separation.

Figure 7 shows the simulation results for zero minimum separation (left) and 10 nm minimum separation (right). The graphs clearly indicate that using the no correlation model can cause serious errors in estimating the conflict probability. This comes as no surprise, because making completely random extractions of the wind speed leads to smaller deviations from the reference path as observed in Sec. III.B. This results in an overestimation of the conflict probability in the cases of zero separation and an underestimation in the case of 10 nm separation. The absolute estimation error reaches 13% in the cases of 45 and 135 deg and 19% in the case of 90 deg.

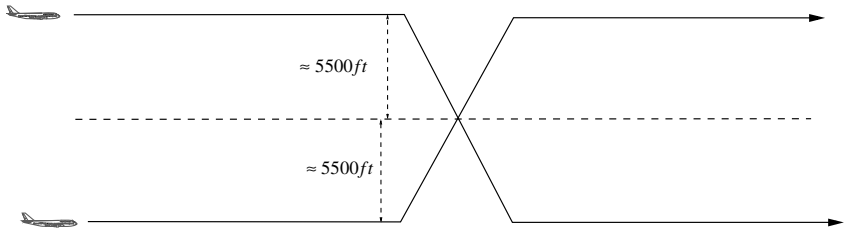

Fig. 11 Conflict scenario with one aircraft climbing and the second descending.

On the other hand, ignoring the cross-correlation structure between the wind encountered by the two aircraft is of small importance only in the case of 90 deg. The reason is that the two aircraft experience two uncorrelated perpendicular wind components, because a change in one wind component will not affect the other. In any other case, the wind experienced by one aircraft can be analyzed into one component parallel to the wind vector of the other aircraft and one perpendicular. This applies in the cases of 45 and 135 deg, where a change in the wind experienced by the first aircraft is correlated with a change in the parallel wind component of the other aircraft. In these cases we observe a completely different pattern, since ignoring the correlation structure leads to larger estimation errors. The case of zero minimum separation and 135 deg crossing angle might seem an exception, but this is because the conflict probability is close to 100%. The absolute estimation error reaches 17% for the case of 45 deg, 8% for the 135 deg crossing angle, and 7% in the case of flight paths crossing at 90 deg, underestimating the conflict probability in the zero separation case and overestimating in the case of 10 nm minimum separation. This observation can be explained by the fact that in the fully correlated model aircraft are more likely to encounter similar wind phenomena, leading to less variances in their relative positions on the horizontal plane. The better estimation in the case of 135 deg compared to 45 deg is because of the larger initial distance of the aircraft.

The results suggest that for level flight both simplified correlation structures should be used with caution, because they can lead to false estimations of aircraft trajectories.

B. Level–Climb and Level–Descent Encounters

Because the level flight scenario covers only a small percentage of conflict cases, we generalize the experiments to three-dimensional conflict scenarios. We start with the case where one of the two aircraft is flying level and the other aircraft is in the climb phase or in the

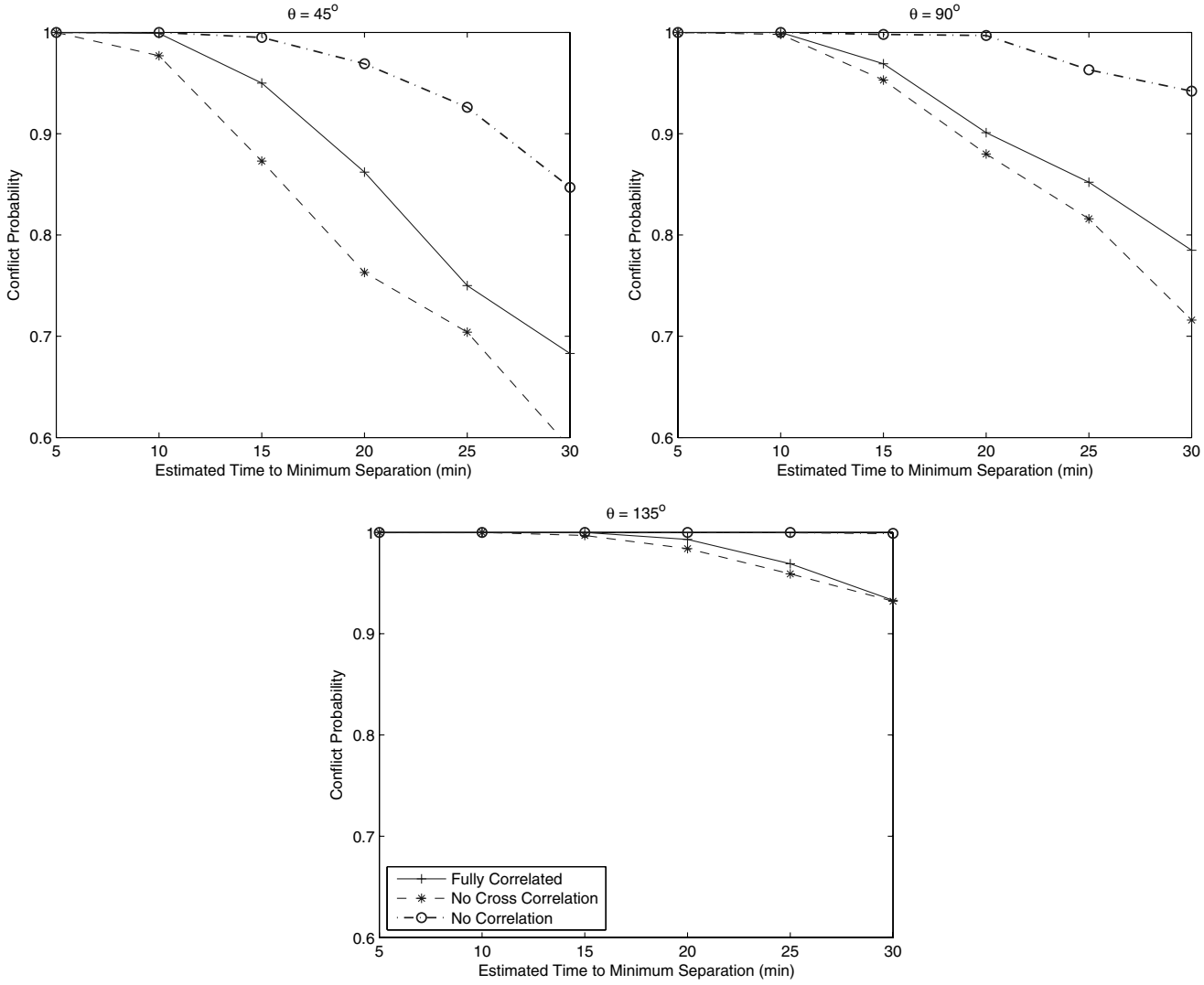

Fig. 12 Effect of wind correlation on conflict probability for the climb–descent scenario.

descent. As suggested in [11], 18% of conflicts happen while one aircraft is climbing and the other is flying level and 22% while one aircraft is descending and the other is flying level.

Since climbing for over 10 min is rare when cruising, our nominal scenario for the climb–level encounter makes the assumption that both aircraft fly level at different altitudes and 5 min before the time of minimum separation, the one flying in lower altitude starts climbing; the climb phase is completed after 10 min (see Fig. 8). In cruising altitudes, an aircraft climbs about 5500 ft in 5 min. Because descent is faster than climb, we will use the same altitude difference for this case as well, requiring about 3 min for an aircraft to descend to the conflict altitude (Fig. 9).

The two aircraft flight plans, as seen from above, look like Fig. 6. We run only simulations with zero minimum separation (horizontal and vertical). Because an analytical solution is more difficult in this case, the flight plans were constructed by running simulations without the presence of wind and measurement errors.

Figure 10 shows the simulation results for the two scenarios. A very interesting fact is that the conflict probabilities of the two conflict scenarios are similar in the cases of 45 and 90 deg. The big difference in the case of 135 deg is explained by the fact that the descending phenomenon is about twice as fast as the climbing one, not allowing the two aircraft to stay for a long time period within the critical vertical distance of 1000 ft.

Once again, the graphs clearly indicate that using a completely uncorrelated model leads to errors in the estimation of the conflict probability, in particular, an overestimation of the conflict probability, producing an absolute error growing with time and reaching to 19%.

The conflict probability is better approximated using the correlation model without the cross correlation of the aircraft wind fields. Nevertheless, in this case as well the conflict probability is not adequately approximated. As in the level conflict scenario, we observe an underestimation of the conflict probability, which, in this case, is bigger for the 45 deg crossing angle and reaches an absolute error of 12%. In the case of 90 deg, as before, we have better results, with the underestimation not growing beyond 6%. The case of 135 deg is an exception, because the conflict probability is very well estimated, but this is because of the very high conflict probability in the case of the climb level (as in the level conflict scenario).

The simulation results indicate that, even in cases where there is a large enough initial vertical distance between the aircraft, there is a benefit to using the full correlation model.

C. Climb–Descent Encounters

This is the most usual case for conflicts in civil aviation [11], as 34% of conflicts are likely to happen with one aircraft in the climb phase and the other one descending. We assume a conflict scenario where both aircraft fly level at altitudes of about 5500 ft above and below the conflict altitude and start climbing and descending a few minutes before the conflict (Fig. 11). The flight plan for each aircraft is the same as in the previous case. Once again, both flight plans pass from exactly the same point (zero nominal minimum separation) after specific times (between 5 and 30 min), and their flight plans intersect at three different angles (45, 90, 135 deg).

Results from the simulations are presented in Fig. 12. As expected, using the no correlation model leads to unacceptably high absolute

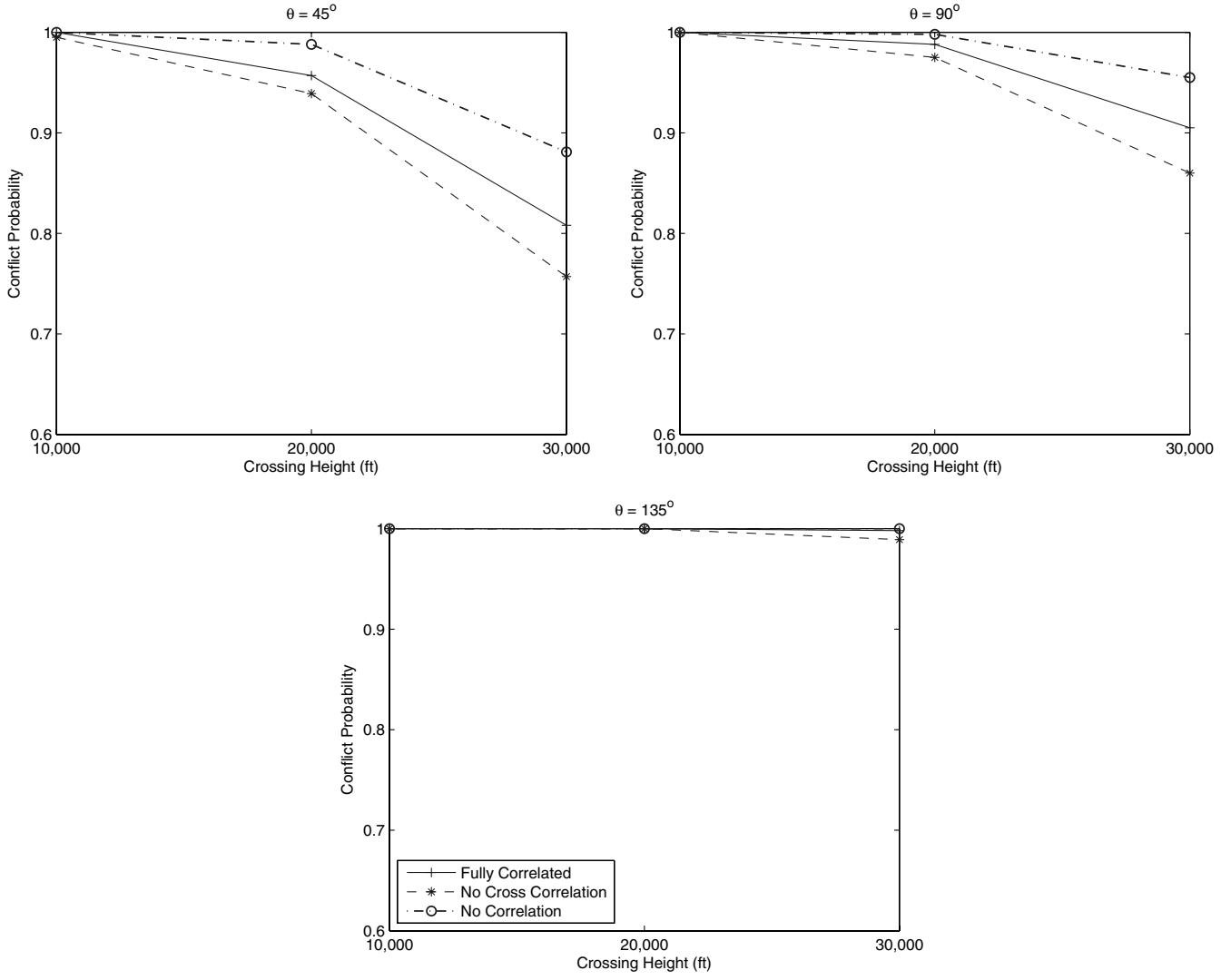

Fig. 13 Effect of wind correlation on conflict probability for the takeoff scenario.

estimation errors (reaching 17%), for the same reasons as before. In the case of the model not including the cross correlation between the aircraft wind fields, for 45 and 90 deg the absolute estimation errors can be as large as 10 and 6%, respectively, while for 135 deg this error is almost zero. This is again explained by the high conflict probability and the large initial distance of the aircraft.

D. Conflicts During Takeoff

In the case where one of the aircraft is taking off, the initial positions of the aircraft have a large vertical distance and we expect the effect of the correlation to be minimal. For simplicity, we consider a case where the aircraft taking off can conflict with another aircraft, flying level at three different altitudes (10,000, 20,000, 30,000 ft). The remaining setup of the simulation is the same (crossing angles, correlation models).

The simulation results are presented in Fig. 13. Once again, the no correlation model cannot estimate precisely the conflict probability, leading to overestimations up to about 8%. The no cross-correlation model on the other hand estimates much better the conflict probability, making underestimation errors (absolute) of no more than 5%. This is because the large initial vertical distance between the aircraft implies a small initial correlation between the wind fields. The error reduces as the crossing angle increases, as in the previous cases.

E. Cumulative Error Estimates

Using statistics from [11], we can combine the results in the previous sections weighting the estimation errors by the probability of each encounter. We then get the formula

$$\epsilon = \frac{0.17 \cdot \epsilon_{l-l} + 0.18 \cdot \epsilon_{c-l} + 0.22 \cdot \epsilon_{d-l} + 0.34 \cdot \epsilon_{c-d}}{0.91} \tag{18}$$

where ϵ stands for the absolute error and the indexes c, d, l for the climbing, descending, and level flight phases, respectively. The exceptional case of the takeoff was not taken into account and in the case of level–level flight, we only used the zero nominal minimum separation encounter.

The errors calculated are shown in Fig. 14. In each plot the dotted line represents the conflict estimation errors in the case where a completely uncorrelated (in time and space) model for the wind field is used. The dashed line represents the conflict estimation errors while using a model not including the cross correlation between the two aircraft wind fields.

For the completely uncorrelated structure, we observe a high estimation error, which can be higher than 15% for crossing angles 45 and 90 deg and more than 7% for crossing angle 135 deg. From these statistics, we conclude that using such a model can severely affect the performance of a conflict probe or a validation tool.

On the other hand, using a structure which does not involve the cross correlation between the two aircraft wind fields leads to errors,

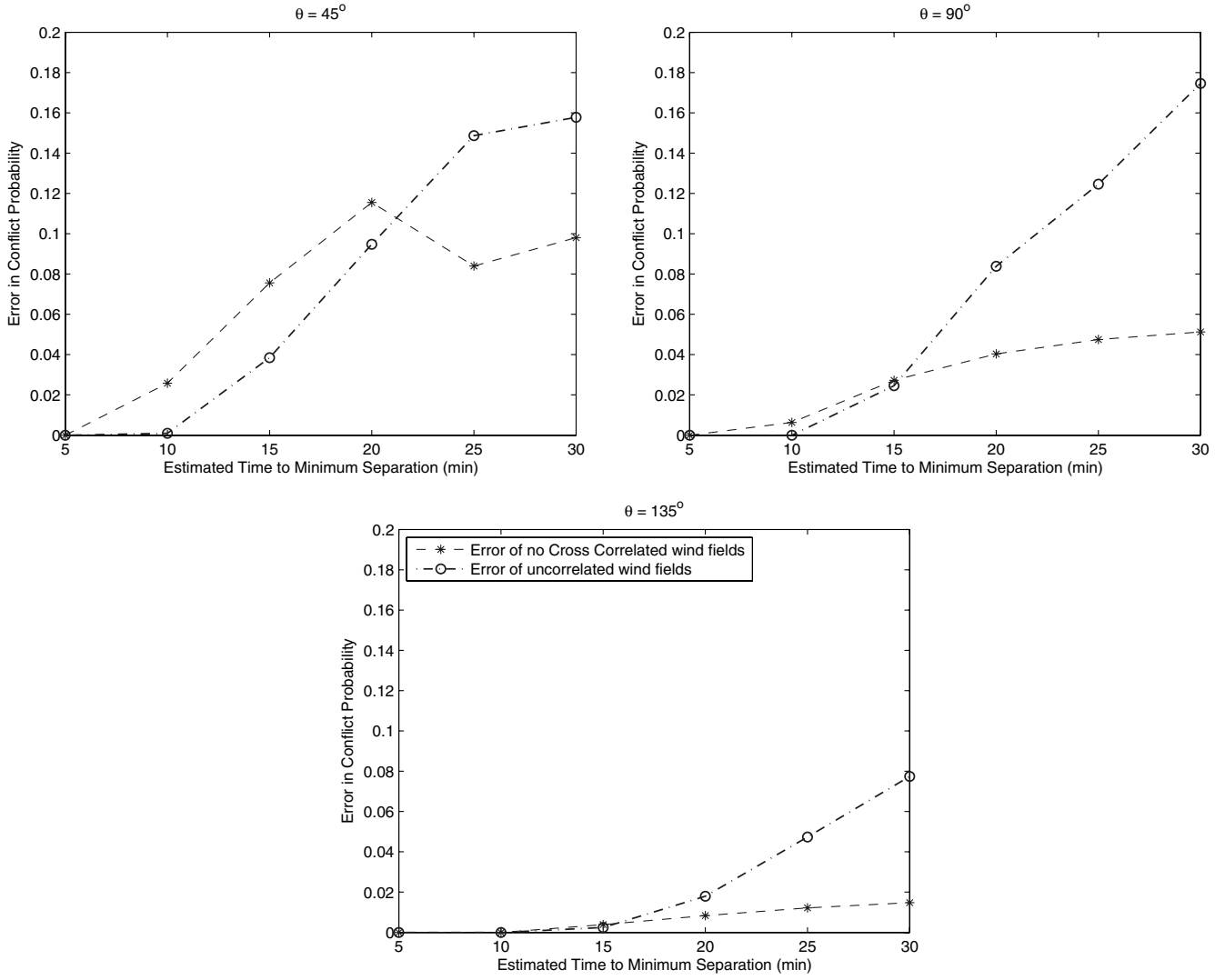

Fig. 14 Estimation errors as a function of time to minimum separation.

which rise to almost 12% in the case of the 45 deg crossing angle, to about 5% in the case of 90 deg, and to no more than 2% in the case of the 135 deg crossing angle. These facts clearly indicate that the use of such a simplified model or other methods (as in [5,13,23]) disregarding the correlation between the wind fields can cause substantial conflict probability estimation errors in the case of 45 and 90 deg crossing angles, while the problem is not severe for 135 deg. The error in this case may increase, however, under different circumstances, for example, flight plans with nonzero nominal minimum separation, treated only for level–level encounters here.

A related study using RUC-1 data [15] suggests that accuracy improvement of weather forecasts is not as important as one would think. RUC-2 has a 40 km horizontal resolution, 40 vertical levels, runs on 1 h assimilation frequency, compared to 60 km horizontal resolution, 25 vertical levels, and 3 h frequency of RUC-1, suggesting 10 times finer forecasts. The effect of the wind correlation structure though is almost the same for the no cross-correlation case and is reduced only about 35% for the completely uncorrelated case.

V. Conclusions

Conflict probability estimation accuracy is critical for the performance of conflict probes and thus, estimation errors should be reduced whenever possible. The simulation results presented in this paper demonstrate that making simplifying assumptions concerning the correlation structure of the wind can affect trajectory prediction results of two-aircraft encounters. Improvements in weather models are reducing the correlation effect, though there is always a significant benefit to using the full spatiotemporal correlation model. Also, because the effect of the correlation cannot be exactly determined and it varies depending on the conflict scenario, inferring the true conflict probability from the estimates of conflict probes obtained under simplifying assumptions is likely to be difficult. Furthermore, temperature and other weather phenomena correlations would result in even higher estimation errors. Further research can include 4-D FMS equipped aircraft, where we expect better performance, since the along-track errors of these aircraft are smaller. We are currently working on Monte Carlo based trajectory prediction and conflict detection and resolution methods that allow one to take into account (and in some cases exploit) the correlation in meteorological forecast errors.

Acknowledgments

This research is supported by Eurocontrol under Contract C20051E/BM/03 and by the European Commission under Project ERASMUS, FP6-TREN-518276.

References

[1] Kahne, S., and Frolow, I., "Air Traffic Management: Evolution with Technology," *IEEE Control Systems Magazine*, Vol. 16, No. 6, 1996, pp. 12–21.

[2] Kuchar, J., and Yang, L., "A Review of Conflict Detection and Resolution Methods," *IEEE Transactions on Intelligent Transportation Systems*, Vol. 1, No. 4, 2000, pp. 179–189.

[3] Glover, W., and Lygeros, J., "A Stochastic Hybrid Model for Air Traffic Control Simulation," *Hybrid Systems: Computation and Control*, edited by R. Alur and G. Pappas, No. 2993 in LNCS, Springer–Verlag, New York, 2004, pp. 372–386.

[4] Lymperopoulos, I., Lygeros, J., and Lecchini, A., "Model Based Aircraft Trajectory Prediction During Takeoff," *AIAA Guidance, Navigation, and Control Conference and Exhibit*, AIAA, Reston, VA, 21–24 Aug. 2006.

[5] Paielli, R. A., "Empirical Test of Conflict Probability Estimation," *2nd USA/Europe Air Traffic Management R&D Seminar*, NASA Ames Research Center, Moffett Field, CA, 1–4 Dec. 1998.

[6] Irvine, R., "A Geometrical Approach to Conflict Probability Estimation," *4th USA/Europe Air Traffic Management R&D Seminar*, Eurocontrol Experimental Center, Brétigny-sur-Orge, France, 3–7 Dec. 2001.

[7] Blin, K., Akian, M., Bonnans, F., Hoffman, E., Martini, C., and Zeghal, K., "A Stochastic Conflict Detection Model Revisited," *AIAA Guidance, Navigation, and Control Conference and Exhibit*, AIAA, Reston, VA, 14–17 Aug. 2000.

[8] Durand, N., and Alliot, J.-M., "Optimal Resolution of En Route Conflicts," *1st USA/Europe Air Traffic Management R&D Seminar*, Centre d'Etudes de la Navigation Aérienne, Toulouse, France, 17–20 June 1997.

[9] Hu, J., Prandini, M., and Sastry, S., "Aircraft Conflict Detection in Presence of a Spatially Correlated Wind Field," *IEEE Transactions on Intelligent Transportation Systems*, Vol. 6, No. 3, 2005, pp. 326–340.

[10] Lecchini, A., Glover, W., Lygeros, J., and Maciejowski, J., "Monte Carlo Optimisation for Conflict Resolution in Air Traffic Control," *IEEE Transactions on Intelligent Transportation Systems*, Vol. 7, No. 4, 2006, pp. 470–482.

[11] Magill, S. A. N., "Trajectory Predictability and Frequency of Conflict-Avoiding Action," *CEAS 10th International Aerospace Conference*, Defence Evaluation and Research Agency, Malvern, U.K., 1997.

[12] Magill, S. A. N., "The Effect of Direct Routing on ATC Capacity," *2nd USA/Europe Air Traffic Management R&D Seminar*, Defence Evaluation and Research Agency, Malvern, U.K., 1–4 Dec. 1998.

[13] Paielli, R., and Erzberger, H., "Conflict Probability Estimation for Free Flight," *Journal of Guidance, Control, and Dynamics*, Vol. 20, No. 3, 1997, pp. 588–596.

[14] Lymperopoulos, I., Lecchini, A., Glover, W., Maciejowski, J., and Lygeros, J., "A Stochastic Hybrid Model for Air Traffic Management Processes," Cambridge University, TR CUED/F-INFENG/TR.572, Department of Engineering, Feb. 2007.

[15] Chaloulos, G., and Lygeros, J., "Wind Uncertainty Correlation and Aircraft Conflict Detection Based on RUC-1 Forecasts," Automatic Control Laboratory, TR AUT07-02, ETH Zurich, Feb. 2007.

[16] Eurocontrol Experimental Center, *User Manual for the Base of Aircraft Data (BADA)*, Eurocontrol Experimental Center, Brétigny-sur-Orge, France, 2004.

[17] Cole, R., Richard, C., Kim, S., and Bailey, D., "An Assessment of the 60 km Rapid Update Cycle (RUC) with Near Real-Time Aircraft Reports," MIT Lincoln Laboratory, TR NASA/A-1, 15 July 1998.

[18] Schwartz, B., Benjamin, S., Green, S., and Jardin, M., "Accuracy of RUC-1 and RUC-2 Wind and Aircraft Trajectory Forecasts by Comparison with ACARS Observations," *Weather and Forecasting*, Vol. 15, No. 3, 2000, pp. 316–326.

[19] Benjamin, S., Schwartz, B., and Cole, R., "Accuracy of ACARS Wind and Temperature Observations Determined by Collocation," *Weather and Forecasting*, Vol. 14, No. 6, 1999, pp. 1032–1038.

[20] Prandini, M., Hu, J., Lygeros, J., and Sastry, S., "A Probabilistic Approach to Aircraft Conflict Detection," *IEEE Transactions on Intelligent Transportation Systems*, Vol. 1, No. 4, 2000, pp. 199–220.

[21] Eurocontrol Experimental Centre, "Navigational Accuracy of Aircraft Equipped with Advanced Navigation Systems," TR EEC 216, EUROCONTROL, June 1998.

[22] Erzberger, H., Paielli, R., Isaacson, D., and Eshow, M., "Conflict Detection and Resolution in the Presence of Prediction Error," *1st USA/Europe Air Traffic Management R&D Seminar*, NASA Ames Research Center, Moffett Field, CA, 17–20 June 1997.

[23] Paielli, R., and, Erzberger, H., "Conflict Probability Estimation Generalized to Non-Level Flight," *Air Traffic Control Quarterly*, Vol. 7, No. 3, 1999, pp. 195–222.